

Combination of Adaptive Neuro Fuzzy Inference System and Machine Learning Algorithm for Recognition of Human Facial Expressions

Dr. B. Dhanalaxmi¹, Dr. B. Madhuravani², Dr. Yeligeti Raju³, Dr. C. Balaswamy⁴, Dr. A. Athiraja⁵, Dr. G. Charles Babu⁶, Dr. T. Samraj Lawrence^{7,*}

Department of CSE, Malla Reddy Institute of Engineering and Technology, Secunderabad, India¹

Department of CSE, MLR Institute of Technology (Autonomous), Hyderabad, India²

Department of CSE, Vignana Bharathi Institute of Technology (Autonomous), Hyderabad, India³

Department of ECE, Sheshadri Rao Gudlavalleru Engineering College, Gudlavalleru, India⁴

Department of CSE (AIML), Bannari Amman Institute of Technology, Sathyamangalam, Erode, India⁵

Department of CSE, Gokaraju Rangaraju Institute of Engineering and Technology, Hyderabad, India⁶

Department of IT-College of Engineering and Technology, Dambi Dollo University, Dambi Dollo, Oromia Region, Ethiopia-260^{7*}

Abstract—A face recognition system's initial three processes are face detection, feature extraction, and facial expression recognition. The initial step of face detection involves colour model skin colour detection, lighting adjustment to achieve uniformity on the face, and morphological techniques to maintain the necessary face region. To extract facial characteristics such the eyes, nose, and mouth, the output of the first step is employed. Third-step methodology using automated face emotion recognition. This study's goal is to apply the Adaptive Neuro Fuzzy Inference System (ANFIS) algorithm to increase the precision of the current face recognition systems. For the purpose of removing noise and unwanted information from the data sets, independent data sets and a pre-processing technique are built in this study based on color, texture, and shape, to determine the features of the face. The output of the three-feature extraction process is given to the ANFIS model as input. By using our training picture data sets, it has already been trained. This model receives a test image as input, then evaluates the three aspects of the input image, and then recognizes the test image based on correlation. The determination of whether input has been authenticated or not is made using fuzzy logic. The proposed ANFIS method is compared to the existing methods such as Minimum Distance Classifier (MDC), Support Vector Machine (SVM), Case Based Reasoning (CBR) with the following quality measure like error rate, accuracy, precision, recall. Finally, the performance is analyzed by combining all feature extractions with existing classification methods such as MDC, KNN (K-Nearest Neighbour), SVM, ANFIS and CBR. Based on the performance of classification techniques, it is observed that the face detection failures are reduced, such that overall accuracy for CBR is 92% and it is 97% in ANFIS.

Keywords—ANFIS; Image processing; face recognition; feature extraction; fuzzy logic

I. INTRODUCTION

Computer vision includes face recognition. Face recognition [1] is a biometric approach for identifying a person based on an image of their face. Biological characteristics are used to identify a person. Human eyes can quickly recognize

people by simply glancing at them, but they have a limited focus span. As a result, a computerized approach for facial recognition is developed. Face recognition [2] is the process of automatically detecting and authenticating a person from a photograph or video. Despite the fact that face recognition has been extensively explored [3], there are still obstacles to overcome a number of issues, including:

- Misalignment.
- Pose Variation.
- Illumination Variation.
- Expression Variation.

The efficacy and precision of face recognition must be improved; hence several approaches must be tested. A method for identifying a person based on their input image is called face recognition. Face recognition can be used on mobile devices due to its adaptability. Face recognition on mobile devices has a variety of disadvantages, such as processing power restrictions, storage space restrictions [4], network bandwidth restrictions, privacy problems, and security issues [5]. On mobile devices, face recognition can be used to identify users, identify social networking sites, and separate individuals. It is well-liked in the marketing and security industries [6]. There are many conventional security apps, including applications for username (identity) and password (credentials) [7]. Passwords can be cracked or detected, making traditional mobile apps easy targets for theft. Contrarily, face recognition apps are more effective than conventional ones because they are more versatile and safer, and they do away with the necessity for the user to remember passwords [8]. The finest biometrics for these devices are face recognition programs because they include cameras. The novelty of the proposed work is we consider the color, shape and texture feature of the image. In existing methods, they are considered any on parameter either color or shape or texture. Machine learning implementation we are using the ANFIS model. This paper's

goal is to introduce a facial recognition system for mobile devices.

This paper is structured as follows: Literature review is presented in Section II. The proposed model is explained in Section III. Results are shown and discussed in Section IV. Finally, the conclusion of the presented work is discussed in Section V.

II. LITERATURE SURVEY

We will go through a handful of the many different types of recognition techniques that exist. Based on the input image, the authors of [9] suggested a face identification system for mobile phones. They did this by developing a number of ROI preprocessing steps, the Viola-Jones approach, and Principal Component Analysis (PCA). The system's goals are to speed up and simplify image searches. A unique application for facial recognition on mobile devices was introduced by the developers of [10] that leverages the Bridge Approach (BA) to speed up processing and makes it possible to use the system from any location with an internet connection. Face detection and feature extraction are done with the OpenCV library; face recognition is done with the WEKA library. The face and eye detection, as well as a set of Region of Interest (ROI) preprocessing, were proposed as part of the design and implementation of a face recognition system for the mobile phone platform by the authors of [11]. The PCA has an accuracy rate of 93.8 percent, and Linear Discriminant Analysis (LDA), which has an accuracy rate of 96 percent, are the recognition techniques used. The use of facial recognition on mobile devices was done by the authors of [12]. The PCA method was used by them for recognition. After using the technique, the accuracy for a given threshold was about 92 percent, and it took 0.35 seconds for a small sample of test photos to identify the person. The authors of [13] developed a facial recognition system in MATLAB and tested it on Direct Region of Interest Device (DROID) mobile devices. It examined various face detection techniques (such as color segmentation and template matching) and provided two

methods for recognition (Eigen & Fisher face). With a computation time of 1.58 seconds on DROID, it has an Eigen face recognition rate of 84.3 percent and a fisher face recognition rate of 94 percent [14].

III. PROPOSED METHOD

In this research work, face recognition is done using image processing, pre-processing, feature extraction, and ANFIS. Input images were collected using digital camera pre-processing technique was used remove the noise. Feature extraction was used to extract the essential feature from the pre-processed output image. The ANFIS was used to recognize the face. Receiver Operating Characteristic (ROC) curve was used to evaluate the proposed system performance.

A. Input Image

Every matrix element in a recorded image is typically referred to as a pixel [15]. Two categories can be used to describe input images taken with a digital camera:

- 1) Testing image
- 2) Training image

Training images and Testing images were obtained using a digital camera for Fig. 1. In this research, we used 16 different data sets. 1600 photos total were used as input, with 1120 images used for the training data set and 480 images used for the testing data (Given in Table I). We are utilizing a jpeg image with dimensions of 256 x 234 pixels.

B. Pre-processing

In this research work, normalization method and soft coring filter were used (shown in Fig. 2). In Fig. 3, Pre-processing is a method used to remove the noise from the input image. Normalization method was used to convert the RGB image into gray scale image using (1) [16].

$$I(x, y, z) = \frac{Gx + Gy + Gz}{3} \quad (1)$$

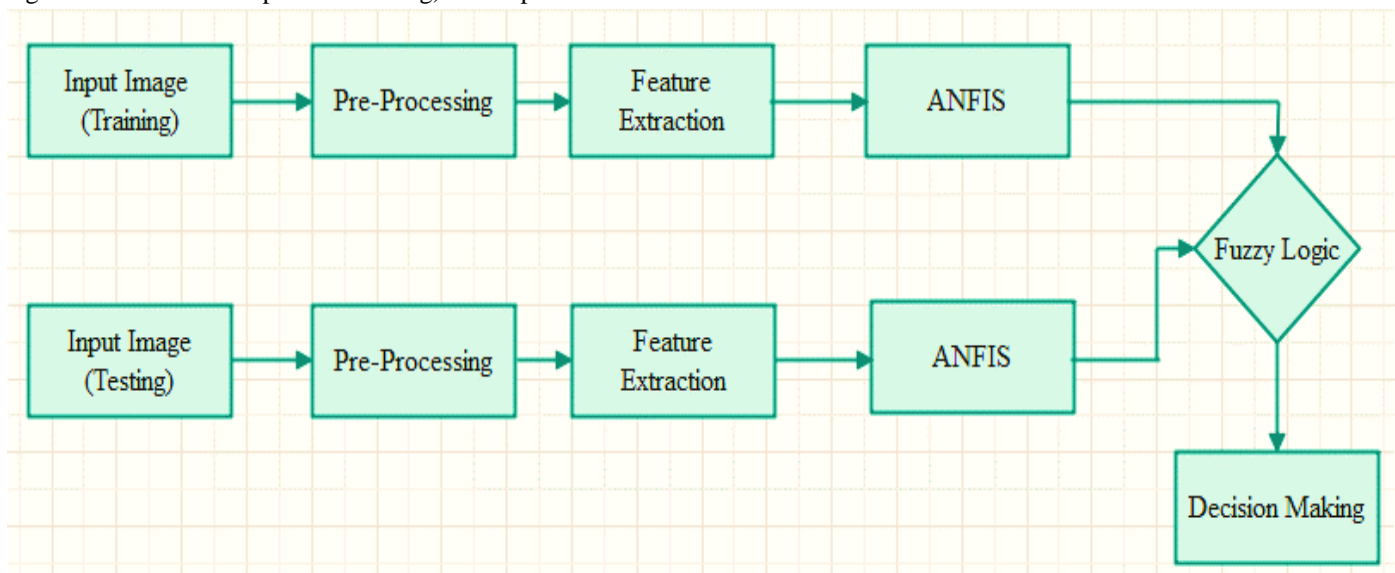


Fig. 1. Block diagram for proposed system

TABLE I. SAMPLE DATABASE

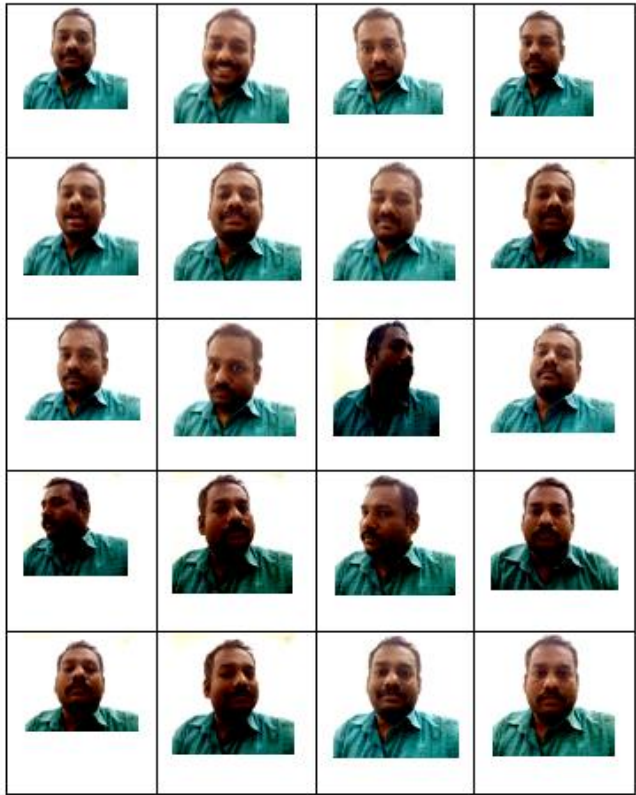


Fig. 2. Pre-processed output image.

The output of the soft coring function was applied after the normalized output picture had been passed through the high pass filter $\alpha(\cdot)$ using equation (4).

$$P(x, y) = Ih(x, y) + \alpha(I(x, y)), \quad (2)$$

where,

$P(x, y)$ – Preprocessed output image

$Ih(x, y)$ – Highpass filter output image

$$Ih(x, y) = I(x, y) - Z(e^{jwx}, e^{jwy}) \quad (3)$$

$Z(e^{jwx}, e^{jwy})$ - High pass filter co-efficient

$\alpha(I(x, y))$ - Soft coring function

$$\alpha(I(x, y)) = m \cdot I(x, y) \left(1 - e^{-\frac{|I(x, y)|}{\tau}}\right) \quad (4)$$

m, τ – Random variables ranges between 0 to 1.

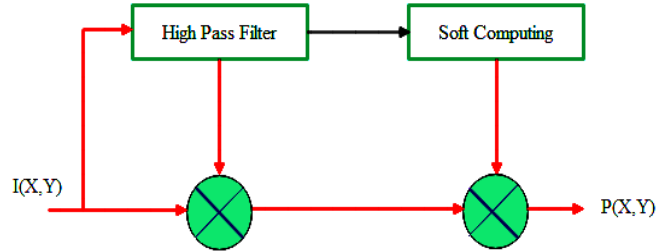


Fig. 3. Soft coring filter.

A nonlinear technique called soft coring filtering is used to remove extraneous data from normalized images [17]. Based on a kernel function that may be executed in the frequency domain, a Gaussian high pass filter is utilized to graphically display the data. With the aid of the sliding windowing technique, the Gaussian high pass filter quickly produces a Fourier transform in two dimensions of convolutions [18].

Gaussian high pass filter was used to remove the noise from the input image using equation (3). To extract the input image's line and edge information, the soft coring kernel function was employed. Two dimensional images were filtered using the soft coring approach, which significantly reduced data loss as compared to the median filtering method. Two step pre-processing method contributes to the quality of the image to be enhanced, reduction of processing time, compensation of illumination, reduction of the shaded background, maintenance of the image contrast and brightness [19]. Median filtering cannot apply for the boundary or edges of the input image to overcome this issue we used soft coring filter.

C. Feature Extraction

1) *Texture feature extraction:* After the preprocessing the images are used for feature extraction. Geometry-based techniques use geometric information as a features measure, such as feature relative locations and sizes of the face components. Kanade [20] devised a method that used a vertical edge map to locate the eyes, mouth, and nose. These procedures necessitate a threshold and may have a negative impact on the final result [21]. Co-occurrences matrix-based technique was used to extract the texture feature using. The following features of co-occurrence matrix can be measured.

- Inertia (contrast).
- Energy.
- Entropy.
- Contrast.

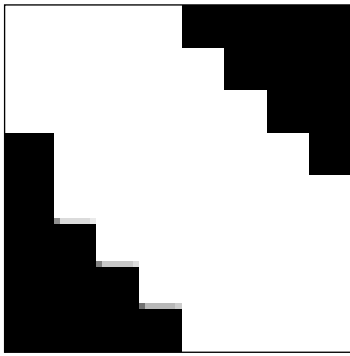


Fig. 4. Texture Feature extraction output image.

The output of the texture feature method is shown in Fig. 4. The element difference moment of order 2 is called as contrast [22]. It has relatively minimum values when maximum values appear in the main diagonal of co-occurrence matrix

$$Contrast = \sum_{g1} \sum_{g2} (g1 - g2)^2 C_{g1 g2} \quad (5)$$

where, $g1$ = grey level value of pixel location at (x,y) ;

$g2$ =grey level value of pixel location at (x,Dx,y,Dy) ;

Dx,Dy =displacement vector of x and y ;

C =co-occurrence matrix

The energy value is calculated by using the following (6). If all values in the co-occurrence matrix are equal, then energy value is maximum.

$$ENERGY = \sum_{g1} \sum_{g2} C_{g1 g2}^2 \quad (6)$$

Entropy is used to calculate the information of the grey level image. To calculate the entropy value the (7) is used:

$$ENTROPY = - \sum_{g1} \sum_{g2} C_{g1 g2} \log_2 C_{g1 g2} \quad (7)$$

2) *Shape features extraction*: To match the found face components, this method uses a previously established standard face pattern template [23]. This makes use of the proper energy function. The facial image with the best match to a template will use the least amount of energy. Y. Zhong et al. [24] adopt this method, which requires prior knowledge of a priori template modelling. It also necessitates additional computing costs, which have a significant impact on its performance [25]. For faster searching speeds and more template matching optimization, genetic algorithms can be utilized. In this research work, we used canny edge detection method for shape feature extraction (output shown in Fig. 5). This method was used to detect wide range of object edges in an image.

3) *Color feature extraction*: In this research work we used threshold-based segmentation as color feature extraction method. Skin color is used to isolate the face in this method [26]. Any non-skin color part of the face is considered a potential for localization of the eyes and/or mouth. Due to the diversity of ethnic backgrounds, this approach performs poorly on facial image datasets. Color feature is extracted by using (8).

$$E(x, y) = \begin{cases} 0 & \text{if } P(x, y) < T1 \\ 1 & \text{if } T1 \leq P(x, y) \leq T2 \\ 0 & \text{if } P(x, y) > T2 \end{cases} \quad (8)$$

where $T1$ –Lower threshold value, $T2$ - Upper threshold value.



Fig. 5. Shape feature extraction output image.

4) *ANFIS (Adaptive Neuro Fuzzy Interface System)*: The outputs of feature extraction methods for colour, texture, and form were fed into the ANFIS. The ANFIS machine learning method, which combines fuzzy logic and neural network methods, is supervised [27]. We are using feed-forward neural networks as a neural network methodology and the Takagi-Sugeno fuzzy logic method as a fuzzy logic method. The architecture of the ANFIS is shown in Fig. 6, which has many layers. Layer 1: In this research work, we used Gaussian membership function. Layer 2: In this layer every node is adaptive, it is labelled as π . The output of this layer is the multiplying result of the first layer as shown in ANFIS architecture, Fig. 6. In this research, the target value is calculated using O R logic. Layer 3: In this layer every node is adaptive, it is labelled as N . The output of this layer is the ratio of firing strength of each node to the sum of all the nodes firing strength. Layer 4: In this layer every node is adaptive. Layer 5: In this layer there is a single node, it is non adaptive and represented as \sum . Layer 6: Output Layer. Six rules make up the Takagi-Sugeno fuzzy model. With ANFIS, the problems with facial detection are overcome. A hybrid learning strategy was used to identify the face utilising the back propagation gradient approach and the least squares method. The nodes in the ANFIS network met the specifications for each tier. IF/THEN rules might build a network realisation in ANFIS. Each layer of the ANFIS network's neurons carried out the same duty [28]. To implement this algorithm, we were used MATLAB software. Fig. 7 and 8 display the ANFIS confusion matrix and colour feature extraction result.

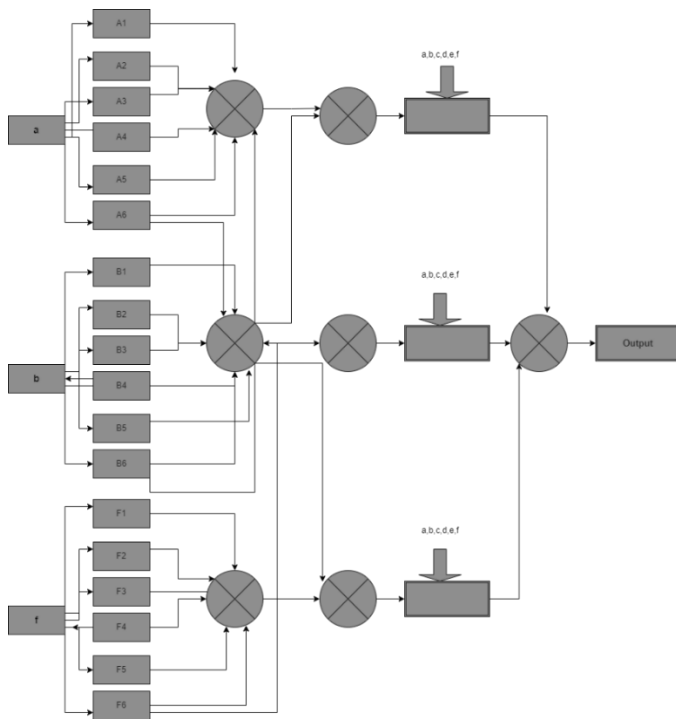


Fig. 6. ANFIS architecture.



Fig. 8. ANFIS output.

5) *Face recognition*: The last procedure in our suggested approach employs the Pearson Correlation Coefficient. Pearson correlation assesses the degree to which two variables are linearly related [29]. We use the Pearson correlation to determine the covariance between a person's features and authorized users' features in the database in order to gain access to the mobile device.

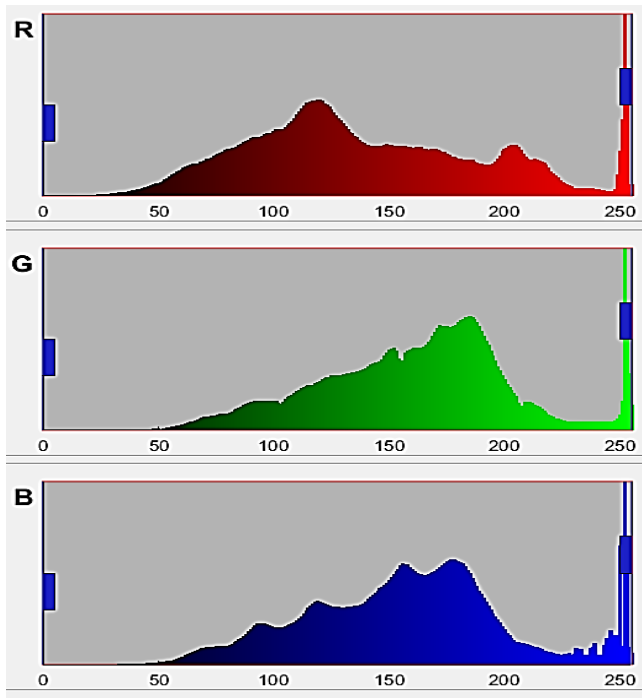


Fig. 7. Color feature extraction output.

If the covariance ratio is equal to or higher than a specific threshold, the system will accept the person as an authorized user; otherwise, the system will deny the access request. The built-in Pearson correlation function in MATLAB is used in this project. We have n "data pairings," where n is the number. The symbol n stands for the bivariate sample n2. The two images A and B have a greater correlation coefficient, which suggests that they are closely related. Based on the covariance rate, we determined whether or not the person is known. If the covariance ratio is equal to or higher than a specific threshold, the system will accept the person as an authorized user; otherwise, the system will deny the access request [30]. It contrasts the 30 measurements of the person requesting access to the system with the measurements of those who have been granted access in the (SQLite) database.

IV. RESULTS

The ROC curve is a graph used to depict the relationship between sensitivity and specificity and to represent the output of a classification system for various threshold values. True Positive Rate (TPR), probability detection, and recall are additional names for sensitivity [31]. Specificity is also known as the False Positive Rate (FPR), the likelihood of a false alert, and fallout. A diagnosis paradigm for classifying instances into groups is the ROC curve. The continuous output is the diagnosis output (real value). The classifier having different boundaries between different classes can be classified by threshold value [32]. The binary classification system is having two classes, one normal cell class which is labelled as positive (P) and other one is abnormal cell class, and it is labelled as negative (N).

The binary classifier has four possible outcomes are

- True Positive (TP).

- False Positive (FP).
- True Negative (TN).
- False Negative (FN).

TABLE II. TRUE POSITIVE AND NEGATIVE VALUES

		Training Image	
		P	N
Testing Image	P	TP	FN
	N	FP	TN

Plotting the cumulative distribution functions of specificity on the x-axis and sensitivity on the y-axis results in the ROC curve. Using (9) and (10) as a basis for actual positive and negative values, determine the sensitivity and specificity values. The following criteria are used to calculate the true positive and negative values, as shown in Table II.

$$Sensitivity = \frac{TP}{(TP+FN)} \quad (9)$$

$$Specificity = \frac{TN}{TN+FP} \quad (10)$$

where, TP- True Positive, TN- True Negative, FN- False Negative, and FP- False Positive.

The examination of ROC curves is a more effective method for choosing an optimization model, class distribution, disease diagnosis, and decision-making. The ROC curve is employed in a variety of fields, including biometrics, machine learning, hazard prediction, radiography, model performance evaluation, and medicine. Based on the diagonal splits in the ROC area, ROC curve analysis is used to identify person [33]. The disease-affected image is represented by the ROC curve above the diagonal, and the disease-free picture is represented by the ROC curve below the diagonal. The threshold value largely determines the ROC curve output, thus choosing the right threshold value will help the analysis of the ROC curve perform better. Fig. 9 displays the ROC curve. Plotting the cumulative distribution functions of specificity on the x-axis and sensitivity on the y-axis results in the ROC curve [34]. The system is performing well and efficiently if the curve in the plot is above the 45-degree slope line. In this research work, we used soft coring filtering method to remove the noise from the input image. The performance of the soft coring filter was compared with median filter based on the quality measure like Mean Square Error (MSE), Peak to Signal Noise Ratio (PSNR), Structural SIMilarity (SSIM), Peak Root mean square Difference (PRD) and Signal Noise Ratio (SNR) [35].

The MSE value was calculated using the following formula.

$$MSE = \frac{1}{MN} \sum_{x=0}^{M-1} \sum_{y=0}^{N-1} [f(x, y) - f^\wedge(x, y)]^2 \quad (11)$$

where f(x,y) – input image; x- row value; y-column value.

The PSNR value was calculated using the following formula.

$$PSNR = 10 \log_{10} \left(\frac{MAX_i^2}{MSE} \right) \quad (12)$$

where MAX_i – Pixel value maximum; MSE-Mean Square Error.

The SSIM value was calculated using the following formula.

$$SSIM(x, y) = \frac{(2\mu_x\mu_y+C1)(2\sigma_{xy}+C2)}{(\mu_x^2+\mu_y^2+C1)(\sigma_x^2+\sigma_y^2+C2)} \quad (13)$$

where μ - mean; σ - variance.

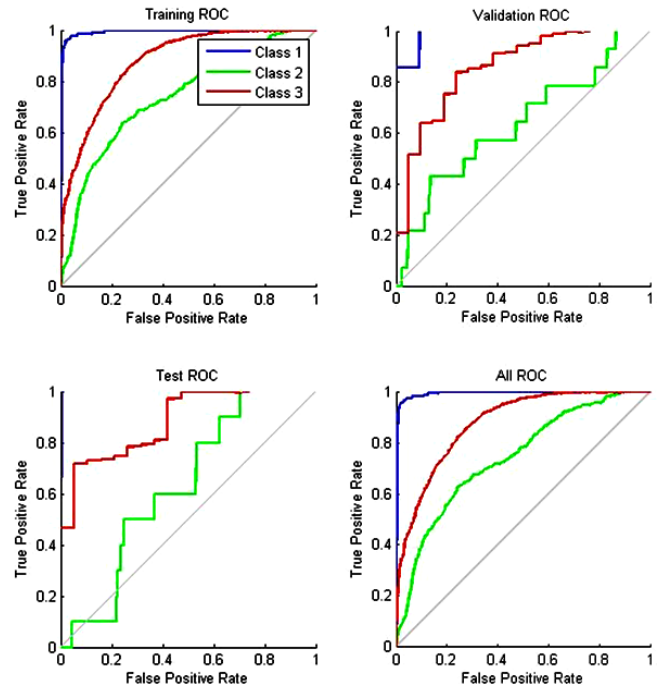


Fig. 9. ROC Output.

The PRD value was calculated using the following formula.

$$PRD = \sqrt{\frac{MSE}{\sum f^2} \times 100} \quad (14)$$

where MSE-Mean Square Error; f-image.

To calculate the SNR value using the following formula

$$SNR = \frac{\sum_{x=0}^{M-1} \sum_{y=0}^{N-1} (f^\wedge(x, y))^2}{\sum_{x=0}^{M-1} \sum_{y=0}^{N-1} [f(x, y) - f^\wedge(x, y)]^2} \quad (15)$$

where f(x,y) – input image; x- row value; y-column value.

Tables III and IV show the performance of filtering technique in terms of MSE, PSNR, SSIM, PRD and SNR. In soft coring filter MSE, SNR and PRD values were low when compared with median filter technique whereas PSNR and SSIM values were high compared with median filter technique [36]. This graph can be used to determine how well filtering methods based on the MSE, PSNR, SSIM, PRD, and SNR perform (shown in Fig. 10 and 11). The MSE, SNR, and PRD values of the median filter were high when compared to the Soft coring filter technique. The median filter's PSNR and SSIM values were poor when compared to the Soft coring filter method. It suggests that when compared to median filters, soft coring filters perform better.

TABLE III. PERFORMANCE ANALYSIS FILTER USING MSE, PSNR AND SSIM

Data Set	Median Filter			Soft Coring Filter		
	MSE	PSNR	SSIM	MSE	PSNR	SSIM
Data set 1	0.0122	30.6193	0.4956	0.0023	41.2563	0.9079
Data set 2	0.0134	30.0458	0.4972	0.0031	41.7865	0.9045
Data set 3	0.0137	30.1246	0.4942	0.0018	41.9658	0.9061
Data set 4	0.0129	30.2148	0.4987	0.0015	41.6587	0.9032
Data set 5	0.0125	30.3127	0.4963	0.0017	41.9623	0.9027
Data set 6	0.0121	30.1248	0.4982	0.0021	41.8865	0.9062
Data set 7	0.0122	30.0458	0.4956	0.4972	41.7865	0.9045
Data set 8	0.0125	30.1246	0.4942	0.0018	41.6587	0.9032
Data set 9	0.0129	30.6193	0.4987	0.0015	41.2563	0.9062
Data set 10	0.0137	30.2148	0.4982	0.0023	41.9658	0.9079
Data set 11	0.0125	30.3127	0.4956	0.0017	41.7865	0.9061
Data set 12	0.0134	30.6193	0.4942	0.0021	41.8865	0.9045
Data set 13	0.0137	30.2148	0.4972	0.4972	41.6587	0.9032
Data set 14	0.0125	30.1246	0.4963	0.0015	41.2563	0.9079
Data set 15	0.0134	30.3127	0.4987	0.0023	41.9623	0.9027
Data set 16	0.0122	30.0458	0.4956	0.0018	41.9658	0.9061

TABLE IV. PERFORMANCE ANALYSIS FILTER USING PRD AND SNR

Data Set	Median Filter		Soft Coring Filter	
	PRD	SNR	PRD	SNR
Data set 1	0.092	4.94	0.043	7.89
Data set 2	0.097	4.87	0.043	7.96
Data set 3	0.098	4.89	0.043	7.35
Data set 4	0.096	4.93	0.043	7.69
Data set 5	0.092	4.23	0.043	7.78
Data set 6	0.095	4.45	0.043	7.63
Data set 7	0.097	4.94	0.043	7.96
Data set 8	0.092	4.89	0.043	7.35
Data set 9	0.098	4.93	0.043	7.69
Data set 10	0.096	4.94	0.043	7.78
Data set 11	0.092	4.45	0.043	7.63
Data set 12	0.095	4.23	0.043	7.89
Data set 13	0.097	4.87	0.043	7.96
Data set 14	0.096	4.94	0.043	7.35
Data set 15	0.092	4.93	0.043	7.78
Data set 16	0.098	4.87	0.043	7.69

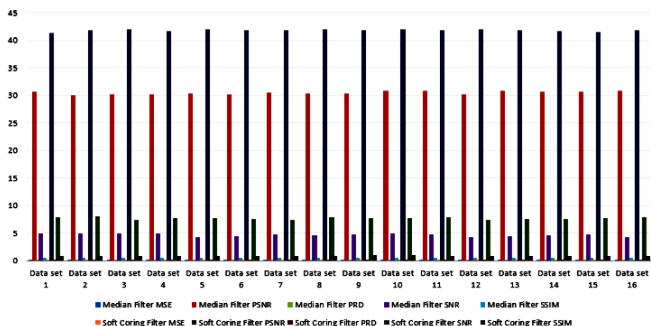


Fig. 10. Performance analysis of preprocessing technique (a) SNR (b) PSNR (c) PRD (d) MSE (e) SSIM.

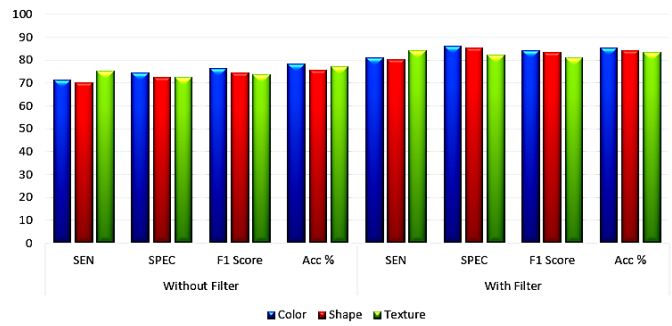
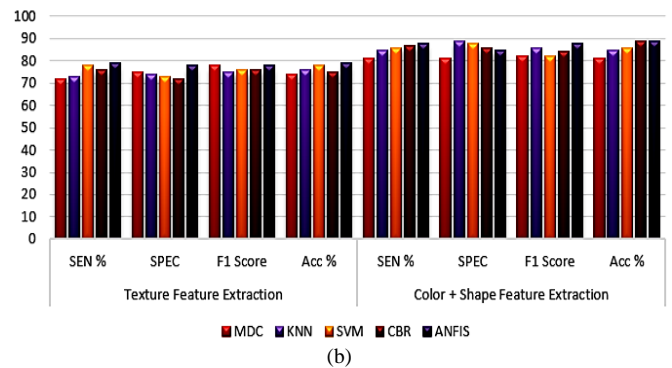
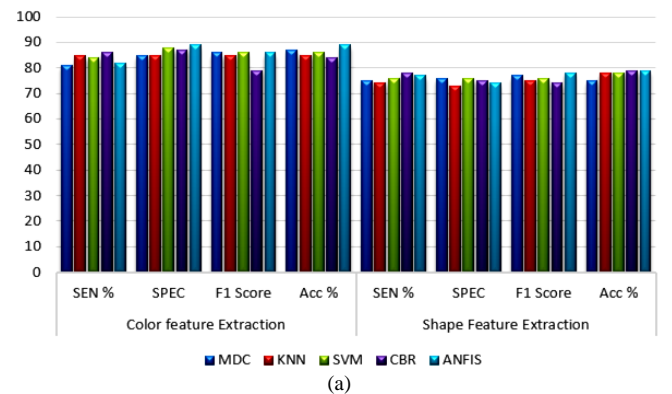


Fig. 11. Performance analyses of Feature extraction techniques.

Table V illustrates the sensitivity, specificity, F1 score, and accuracy of the feature extraction approach. In Fig. 12, color, shape, and texture were quantified using feature extraction techniques with and without filters for these four metrics. With the filter, the sensitivity values were 81.25, 80.26, and 84.36. Other feature extraction methods have lower sensitivity than the texture feature extraction approach. With the filter, the specificity values were 86.23, 85.32, and 82.34. Other feature extraction methods have lower specificity than the colour feature extraction approach [37-38]. The F1 score after applying the filter was 84.35, 83.56, and 81.26. In comparison to other feature extraction techniques, colour feature extraction produced a higher F1 score. There were three different filter accuracy values: 85.26, 84.35, and 83.28. Compared to other feature extraction techniques, the colour feature extraction method offered greater accuracy.



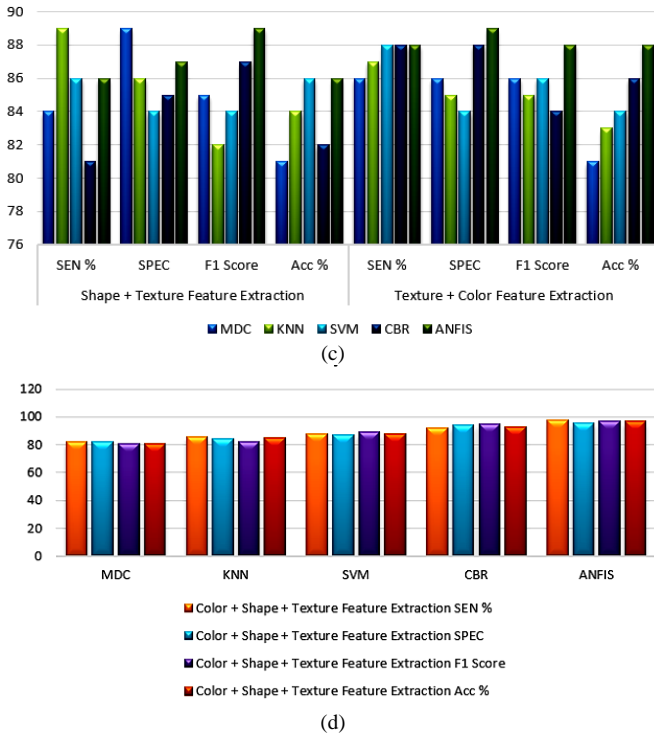


Fig. 12. (a),(b),(c),(d) Performance analysis of classification.

TABLE V. FEATURE EXTRACTION ANALYSIS

Technique	Without Filter %				With Filter %			
	SEN	SPEC	FI	Acc	SEN	SPEC	FI	Acc
Color	71.21	74.36	76.28	78.54	81.25	86.23	84.35	85.26
Shape	70.32	72.36	74.35	75.63	80.26	85.32	83.56	84.35
Texture	75.36	72.36	73.62	77.25	84.36	82.34	81.26	83.28

From Tables VI to IX, it was concluded that classification strategies that integrated feature extraction approaches with values of attributes like sensitivity, specificity, F1 score, and accuracy generated better results. To recognize faces, three approaches were used: assessing the performance of colour, shape, and texture feature extractions separately, then combining (colour and shape), (shape and texture), and (texture and colour), and lastly merging all feature extraction methods (colour, shape, and texture). The fusion of colour, shape, and texture feature extraction methodology produced more accuracy than earlier feature extraction techniques, as seen in Fig. 12 [39]. Accuracy values for the MDC, KNN, SVM, CBR, and ANFIS techniques are 81, 85, 88, 93, and 97, respectively.

The overall performance of several classification algorithms used for facial recognition classification in terms of execution time is shown in Table X and Fig. 13. ANFIS performed faster than the other categorization algorithms in a comparison. Each data set took 36, 34, 35, 32, 34, 33, 34, 31, 32, 34, 35, and 36 seconds to execute in seconds. The total effectiveness of several classification algorithms utilized for face recognition categorization is shown in Table XI and Fig. 14. According to a comparison of classification methods, ANFIS had higher accuracy than all other methods, with 97.67

percent, 97.45 percent, 97.56 percent, 97.54 percent, 97.61 percent, 97.43 percent, 97.36 percent, 97.63 percent, 97.72 percent, 97.68 percent, 97.28 percent, 97.34 percent, 97.52 percent, 97.62 percent, and 97.48 percent. The average number of iteration performance measures employed is shown in Table XII and Fig. 15. According to a comparison of categorization techniques, ANFIS had the lowest average number of iterations of all methods, with 39, 38, 37, 37, 39, 38, 38, 37, 37, 36, 38, 37, 36, 37, 38 and 36 of data sets.

TABLE VI. CLASSIFICATION METHOD USING COLOR FEATURE EXTRACTION AND SHAPE FEATURE EXTRACTION

Technique	Color feature Extraction %				Shape Feature Extraction %			
	SEN	SPEC	FI	Acc	SEN	SPEC	FI	Acc
MDC	81	85	86	87	75	76	77	75
KNN	85	85	85	85	74	73	75	78
SVM	84	88	86	86	76	76	76	78
CBR	86	87	79	84	78	75	74	79
ANFIS	82	89	86	89	77	74	78	79

TABLE VII. CLASSIFICATION METHOD USING TEXTURE FEATURE EXTRACTION AND COLOR + SHAPE FEATURE EXTRACTION

Technique	Texture Feature Extraction %				Color + Shape Feature Extraction %			
	SEN	SPEC	FI	Acc	SEN	SPEC	FI	Acc
MDC	72	75	78	74	81	81	82	81
KNN	73	74	75	76	85	89	86	85
SVM	78	73	76	78	86	88	82	86
CBR	76	72	76	75	87	86	84	89
ANFIS	79	78	78	79	88	85	88	89

TABLE VIII. CLASSIFICATION METHOD USING TEXTURE + SHAPE FEATURE EXTRACTION AND TEXTURE + COLOR FEATURE EXTRACTION

Technique	Shape + Texture Feature Extraction %				Texture + Color Feature Extraction %			
	SEN	SPEC	FI	Acc	SEN	SPEC	FI	Acc
MDC	84	89	85	81	86	86	86	81
KNN	89	86	82	84	87	85	85	83
SVM	86	84	84	86	88	84	86	84
CBR	81	85	87	82	88	88	84	86
ANFIS	86	87	89	86	88	89	88	88

TABLE IX. CLASSIFICATION METHOD USING COLOR + SHAPE + TEXTURE FEATURE EXTRACTION

Technique	Color + Shape + Texture Feature Extraction %			
	SEN	SPEC	FI Score	Acc
MDC	82	82	81	81
KNN	86	84	82	85
SVM	88	87	89	88
CBR	92	94	95	93
ANFIS	98	96	97	97

TABLE XI. PERFORMANCE ANALYSIS BASED ON EXECUTION TIME

Data set	Execution Time (seconds)				
	MDC	KNN	SVM	CBR	ANFIS
Data set 1	58	52	38	34	36
Data set 2	57	51	36	35	34
Data set 3	58	52	37	33	35
Data set 4	56	50	36	33	32
Data set 5	57	51	38	34	34
Data set 6	55	52	37	35	33
Data set 7	57	52	38	34	32
Data set 8	58	51	36	35	34
Data set 9	56	52	37	34	36
Data set 10	57	52	36	35	34
Data set 11	55	51	36	33	35
Data set 12	58	52	38	35	32
Data set 13	56	50	36	33	34
Data set 14	57	51	37	33	33
Data set 15	58	52	36	34	32
Data set 16	57	52	36	34	34

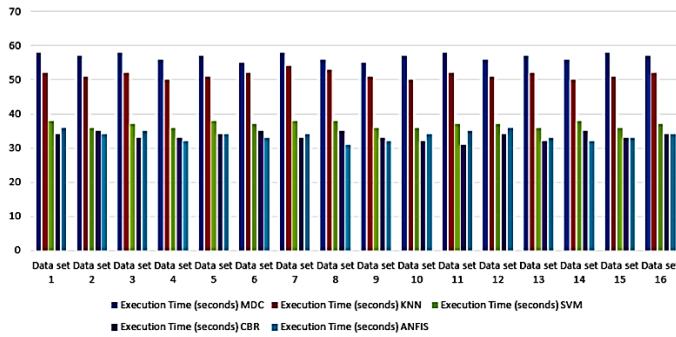


Fig. 13. Performance analysis based on Execution Time

TABLE XII. PERFORMANCE ANALYSIS BASED ON ACCURACY

Data set	Accuracy (%)				
	MDC	KNN	SVM	CBR	ANFIS
Data set 1	82.36	85.25	88.21	92.86	97.67
Data set 2	81.86	85.65	88.86	92.72	97.45
Data set 3	82.39	85.39	88.27	92.79	97.56
Data set 4	81.57	85.76	88.38	92.27	97.54
Data set 5	82.56	85.28	88.74	92.43	97.61
Data set 6	82.24	85.78	88.57	92.62	97.43
Data set 7	81.86	85.65	88.86	92.79	97.45
Data set 8	82.39	85.39	88.27	92.27	97.56
Data set 9	81.57	85.76	88.38	92.86	97.54
Data set 10	82.39	85.28	88.21	92.72	97.61
Data set 11	81.57	85.76	88.86	92.79	97.45
Data set 12	82.56	85.28	88.27	92.79	97.56
Data set 13	82.24	85.78	88.38	92.27	97.54
Data set 14	82.36	85.25	88.21	92.43	97.45
Data set 15	81.86	85.65	88.86	92.62	97.56
Data set 16	82.39	85.39	88.27	92.79	97.54

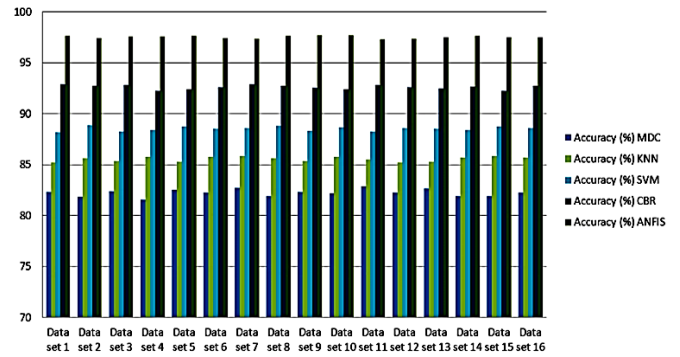


Fig. 14. Performance analysis based on accuracy

TABLE XIII. PERFORMANCE ANALYSIS BASED ON AVERAGE NUMBER OF ITERATIONS

Data set	Average Number of iterations				
	MDC	KNN	SVM	CBR	ANFIS
Data set 1	102	86	74	52	39
Data set 2	101	88	72	56	38
Data set 3	103	89	73	55	37
Data set 4	104	87	71	53	37
Data set 5	102	86	74	54	39
Data set 6	101	84	74	51	38
Data set 7	101	88	73	55	38
Data set 8	103	89	71	53	37
Data set 9	104	87	74	54	37
Data set 10	101	89	73	55	39
Data set 11	103	87	71	53	38
Data set 12	104	86	74	54	37
Data set 13	101	84	74	51	39
Data set 14	103	89	73	55	38
Data set 15	104	87	71	53	37
Data set 16	102	86	74	55	37

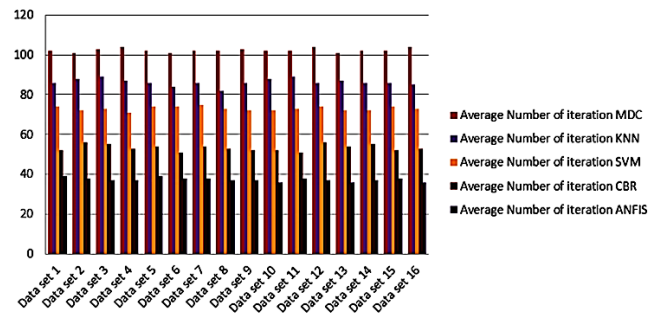


Fig. 15. Performance analysis based on average number of iterations

The overall performance of precision for various classification techniques utilised for the classification of data sets is shown in Table XIII and Fig. 16. According to a comparison of classification methods, ANFIS has higher precision than all other approaches, with precision values for every data set of 97.23%, 97.11%, 97.15%, 97.21%, 97.21%,

97.18%, 97.16%, 97.27%, 97.26%, 97.11%, 97.21%, 97.23%, 97.24%, 97.27%, and 97.28%. The overall recall performance of various classification techniques utilised for classifying data sets is shown in Table XIV and Fig. 17 respectively. Upon comparative analysis of classification methods, ANFIS had higher recall above all other methods that was 96.67%, 96.58%, 96.29%, 96.42%, 96.78%, 96.63%, 96.74%, 96.76%, 96.28%, 96.39%, 96.74%, 96.26%, 96.58%, 96.59%, 96.96% and 96.76% for each data sets.

TABLE XIV. PERFORMANCE ANALYSIS BASED ON PRECISION

Data set	Precision				
	MDC	KNN	SVM	CBR	ANFIS
Data set 1	84.75	86.32	89.56	91.58	97.23
Data set 2	84.56	86.24	89.62	91.56	97.11
Data set 3	84.36	86.31	89.58	91.54	97.15
Data set 4	84.45	86.74	89.54	91.64	97.21
Data set 5	84.63	86.32	89.56	91.62	97.18
Data set 6	84.82	86.72	89.53	91.58	97.16
Data set 7	84.56	86.24	89.62	91.56	97.11
Data set 8	84.36	86.31	89.58	91.54	97.15
Data set 9	84.45	86.74	89.54	91.64	97.21
Data set 10	84.63	86.32	89.56	91.62	97.18
Data set 11	84.56	86.24	89.62	91.58	97.16
Data set 12	84.36	86.31	89.58	91.56	97.11
Data set 13	84.45	86.74	89.54	91.54	97.15
Data set 14	84.63	86.32	89.56	91.64	97.21
Data set 15	84.56	86.24	89.62	91.62	97.18
Data set 16	84.45	86.74	89.54	91.54	97.15

Data set 9	83.24	85.18	87.46	90.80	96.29
Data set 10	83.22	85.13	87.36	90.85	96.42
Data set 11	83.28	85.11	87.42	90.84	96.78
Data set 12	83.21	85.16	87.39	90.87	96.63
Data set 13	83.26	85.12	87.46	90.88	96.67
Data set 14	83.24	85.16	87.36	90.80	96.58
Data set 15	83.22	85.18	87.42	90.85	96.29
Data set 16	83.28	85.13	87.39	90.84	96.42

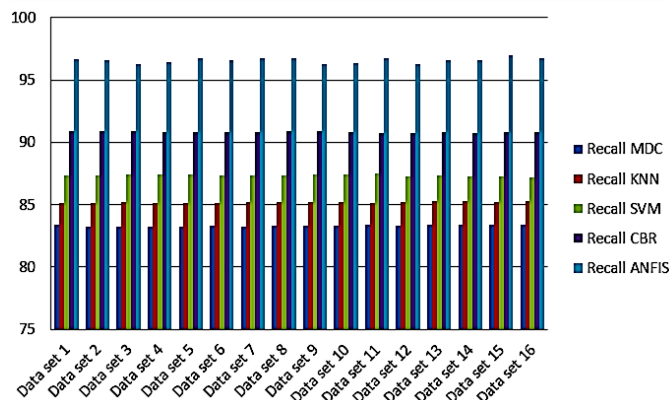


Fig. 17. Performance analysis based on recall

Table XV and Fig. 18 show the overall performance based on error rate of different classification technique employed for classification of data sets. Upon comparative analysis of classification methods, ANFIS had low error rate above all other methods that was 0.086, 0.074, 0.083, 0.056, 0.064, 0.073, 0.084, 0.074, 0.059, 0.065, 0.072, 0.089, 0.085, 0.086, 0.071 and 0.087 for each data set.

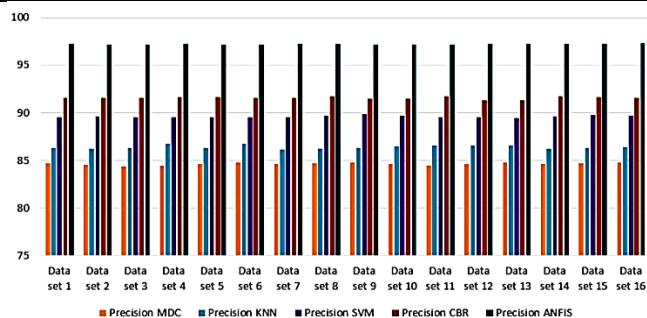


Fig. 16. Performance analysis based on Precision

TABLE XV. PERFORMANCE ANALYSIS BASED ON RECALL

Data set	Recall				
	MDC	KNN	SVM	CBR	ANFIS
Data set 1	83.36	85.12	87.36	90.89	96.67
Data set 2	83.21	85.16	87.38	90.87	96.58
Data set 3	83.26	85.18	87.42	90.88	96.29
Data set 4	83.24	85.13	87.39	90.80	96.42
Data set 5	83.22	85.11	87.46	90.85	96.78
Data set 6	83.28	85.16	87.36	90.84	96.63
Data set 7	83.21	85.12	87.42	90.87	96.67
Data set 8	83.26	85.16	87.39	90.88	96.58

TABLE XVI. PERFORMANCE ANALYSIS BASED ON ERROR RATE

Data set	Error Rate				
	MDC	KNN	SVM	CBR	ANFIS
Data set 1	0.524	0.436	0.286	0.213	0.086
Data set 2	0.578	0.431	0.272	0.217	0.074
Data set 3	0.562	0.486	0.262	0.214	0.083
Data set 4	0.573	0.463	0.253	0.219	0.056
Data set 5	0.548	0.456	0.282	0.216	0.064
Data set 6	0.545	0.448	0.269	0.215	0.073
Data set 7	0.524	0.486	0.253	0.217	0.086
Data set 8	0.578	0.463	0.282	0.214	0.074
Data set 9	0.562	0.456	0.269	0.219	0.083
Data set 10	0.573	0.448	0.253	0.216	0.056
Data set 11	0.548	0.486	0.282	0.215	0.064
Data set 12	0.545	0.463	0.269	0.217	0.073
Data set 13	0.524	0.456	0.253	0.214	0.086
Data set 14	0.578	0.448	0.282	0.219	0.074
Data set 15	0.562	0.486	0.269	0.216	0.083
Data set 16	0.573	0.463	0.253	0.215	0.056

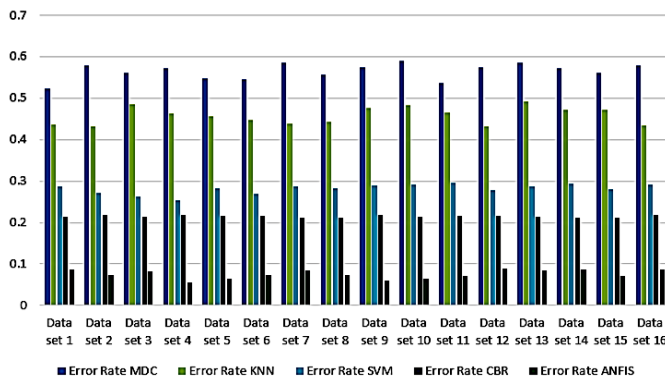


Fig. 18. Performance analysis based on error rate

V. CONCLUSION

Face Detection is required as a preprocessing procedure in a workflow for a variety of applications such as active presence analysis, recognition, and reidentification. In the past, numerous research in the area of face detection were conducted, and multiple robust methods were suggested and tested on diverse datasets. These approaches are also used in a variety of applications. Despite the fact that this domain appears to be rather old and that considerable work has obviously gone into it, there is still opportunity for development. Previous research has focused on challenges such as face positions, emotions, picture scales, and occlusions, with promising results. Work on advanced topics such as low-resolution pictures, suggested anchoring, scale-invariance of models, and model size reduction has been investigated in recent years, with many solutions given. In this article, we will cover the most recent papers in this field, the difficulties they address, and the technologies they employ. The Adaptive Neuro Fuzzy Inference System (ANFIS) method was designed to overcome this problem. In classification techniques like MDC, KNN, SVM, CBR, ANFIS; The performance of ANFIS resulted in better recognition of face. The proposed research method was compared with the existing methods such as MDC, KNN and SVM which proved to provide better accuracy than the latter. CBR accuracy value were 92% and it is 97% in ANFIS. The performance of proposed system was analysed using the following quality measure like execution time, accuracy, F1 score, precision, recall, iteration and error rate ANFIS resulted in better performance compared to other existing system. The limitation of the proposed system is we were used MATLAB software, it needs more memory space to run this project. In future we will try to implement this project in opensource software's like Open CV.

REFERENCES

[1] L. S. Luevano, L. Chang, H. Méndez-Vázquez, Y. Martínez-Díaz and M. González-Mendoza, "A Study on the Performance of Unconstrained Very Low Resolution Face Recognition: Analyzing Current Trends and New Research Directions," in *IEEE Access*, vol. 9, pp. 75470-75493, 2021, doi: 10.1109/ACCESS.2021.3080712.

[2] R. He, J. Cao, L. Song, Z. Sun and T. Tan, "Adversarial Cross-Spectral Face Completion for NIR-VIS Face Recognition," in *IEEE Transactions on Pattern Analysis and Machine Intelligence*, vol. 42, no. 5, pp. 1025-1037, 1 May 2020, doi: 10.1109/TPAMI.2019.2961900.

[3] M. Luo, J. Cao, X. Ma, X. Zhang and R. He, "FA-GAN: Face Augmentation GAN for Deformation-Invariant Face Recognition," in

IEEE Transactions on Information Forensics and Security, vol. 16, pp. 2341-2355, 2021, doi: 10.1109/TIFS.2021.3053460.

[4] Z. An, W. Deng, J. Hu, Y. Zhong and Y. Zhao, "APA: Adaptive Pose Alignment for Pose-Invariant Face Recognition," in *IEEE Access*, vol. 7, pp. 14653-14670, 2019, doi: 10.1109/ACCESS.2019.2894162.

[5] Stanko I. The Architectures of Geoffrey Hinton. In: Skansi S. (eds) *Guide to Deep Learning Basics*. Springer, Cham, 2020.

[6] Xiangbing Zhou, Hongjiang Ma, Jianggang Gu, Huiling Chen, Wu Deng, Parameter adaptation-based ant colony optimization with dynamic hybrid mechanism, *Engineering Applications of Artificial Intelligence*, Volume 114, 2022, 105139, ISSN 0952-1976, <https://doi.org/10.1016/j.engappai.2022.105139>.

[7] F. Liu, Q. Zhao, X. Liu and D. Zeng, "Joint Face Alignment and 3D Face Reconstruction with Application to Face Recognition," in *IEEE Transactions on Pattern Analysis and Machine Intelligence*, vol. 42, no. 3, pp. 664-678, 1 March 2020, doi: 10.1109/TPAMI.2018.2885995.

[8] Buciu, I., & Gacsadi, A., "Biometrics systems and technologies: a survey", *International Journal of Computers Communications & Control*, 11(3), 315-330, 2016.

[9] J. Zhao, L. Xiong, J. Li, J. Xing, S. Yan and J. Feng, "3D-Aided Dual-Agent GANs for Unconstrained Face Recognition," in *IEEE Transactions on Pattern Analysis and Machine Intelligence*, vol. 41, no. 10, pp. 2380-2394, 1 Oct. 2019, doi: 10.1109/TPAMI.2018.2858819.

[10] W. Hu and H. Hu, "Domain Discrepancy Elimination and Mean Face Representation Learning for NIR-VIS Face Recognition," in *IEEE Signal Processing Letters*, vol. 28, pp. 2068-2072, 2021, doi: 10.1109/LSP.2021.3116861.

[11] Wu Deng, Hongcheng Ni, Yi Liu, Huiling Chen, Huimin Zhao, An adaptive differential evolution algorithm based on belief space and generalized opposition-based learning for resource allocation, *Applied Soft Computing*, Volume 127, 2022, 109419, ISSN 1568-4946, <https://doi.org/10.1016/j.asoc.2022.109419>.

[12] A. Sepas-Moghaddam, A. Etemad, F. Pereira and P. L. Correia, "CapsField: Light Field-Based Face and Expression Recognition in the Wild Using Capsule Routing," in *IEEE Transactions on Image Processing*, vol. 30, pp. 2627-2642, 2021, doi: 10.1109/TIP.2021.3054476.

[13] J. Zhao, S. Yan and J. Feng, "Towards Age-Invariant Face Recognition," in *IEEE Transactions on Pattern Analysis and Machine Intelligence*, vol. 44, no. 1, pp. 474-487, 1 Jan. 2022, doi: 10.1109/TPAMI.2020.3011426.

[14] J. Chen, J. Chen, Z. Wang, C. Liang and C. -W. Lin, "Identity-Aware Face Super-Resolution for Low-Resolution Face Recognition," in *IEEE Signal Processing Letters*, vol. 27, pp. 645-649, 2020, doi: 10.1109/LSP.2020.2986942.

[15] J. Y. Choi and B. Lee, "Ensemble of Deep Convolutional Neural Networks With Gabor Face Representations for Face Recognition," in *IEEE Transactions on Image Processing*, vol. 29, pp. 3270-3281, 2020, doi: 10.1109/TIP.2019.2958404.

[16] H. Yang and X. Han, "Face Recognition Attendance System Based on Real-Time Video Processing," in *IEEE Access*, vol. 8, pp. 159143-159150, 2020, doi: 10.1109/ACCESS.2020.3007205.

[17] D. Liu, X. Gao, N. Wang, J. Li and C. Peng, "Coupled Attribute Learning for Heterogeneous Face Recognition," in *IEEE Transactions on Neural Networks and Learning Systems*, vol. 31, no. 11, pp. 4699-4712, Nov. 2020, doi: 10.1109/TNNLS.2019.2957285.

[18] L. He, H. Li, Q. Zhang and Z. Sun, "Dynamic Feature Matching for Partial Face Recognition," in *IEEE Transactions on Image Processing*, vol. 28, no. 2, pp. 791-802, Feb. 2019, doi: 10.1109/TIP.2018.2870946.

[19] J. Neves and H. Proença, "'A Leopard Cannot Change Its Spots': Improving Face Recognition Using 3D-Based Caricatures," in *IEEE Transactions on Information Forensics and Security*, vol. 14, no. 1, pp. 151-161, Jan. 2019, doi: 10.1109/TIFS.2018.2846617.

[20] I. Adjabi et al., "Past Present and Future of Face Recognition: A Review", *Electronics*, vol. 9, no. 8, pp. 1188, 2020.

[21] S. Hong and J. Ryu, "Unsupervised Face Domain Transfer for Low-Resolution Face Recognition," in *IEEE Signal Processing Letters*, vol. 27, pp. 156-160, 2020, doi: 10.1109/LSP.2019.2963001.

- [22] H. Chen, F. Miao, Y. Chen, Y. Xiong and T. Chen, "A Hyperspectral Image Classification Method Using Multifeature Vectors and Optimized KELM," in *IEEE Journal of Selected Topics in Applied Earth Observations and Remote Sensing*, vol. 14, pp. 2781-2795, 2021, doi: 10.1109/JSTARS.2021.3059451.
- [23] A. Maafiri, O. Elharrouss, S. Rfifi, S. A. Al-Maadeed and K. Chougali, "DeepWTPCA-L1: A New Deep Face Recognition Model Based on WTPCA-L1 Norm Features," in *IEEE Access*, vol. 9, pp. 65091-65100, 2021, doi: 10.1109/ACCESS.2021.3076359.
- [24] Y. Zhang, I. W. Tsang, J. Li, P. Liu, X. Lu and X. Yu, "Face Hallucination With Finishing Touches," in *IEEE Transactions on Image Processing*, vol. 30, pp. 1728-1743, 2021, doi: 10.1109/TIP.2020.3046918.
- [25] A. -C. Tsai, Y. -Y. Ou, W. -C. Wu and J. -F. Wang, "Integrated Single Shot Multi-Box Detector and Efficient Pre-Trained Deep Convolutional Neural Network for Partially Occluded Face Recognition System," in *IEEE Access*, vol. 9, pp. 164148-164158, 2021, doi: 10.1109/ACCESS.2021.3133446.
- [26] Q. Duan and L. Zhang, "Look More Into Occlusion: Realistic Face Frontalization and Recognition With BoostGAN," in *IEEE Transactions on Neural Networks and Learning Systems*, vol. 32, no. 1, pp. 214-228, Jan. 2021, doi: 10.1109/TNNLS.2020.2978127.
- [27] J. Liu, Q. Li, M. Liu and T. Wei, "CP-GAN: A Cross-Pose Profile Face Frontalization Boosting Pose-Invariant Face Recognition," in *IEEE Access*, vol. 8, pp. 198659-198667, 2020, doi: 10.1109/ACCESS.2020.3033675.
- [28] H. B. Bae, T. Jeon, Y. Lee, S. Jang and S. Lee, "Non-Visual to Visual Translation for Cross-Domain Face Recognition," in *IEEE Access*, vol. 8, pp. 50452-50464, 2020, doi: 10.1109/ACCESS.2020.2980047.
- [29] W. Qiao, B. Chen, J. Zhao and S. Guo, "Face Recognition Based on CD-RBM and BM-ILM", *Journal of Physics: Conference Series*, vol. 1802, no. 3, pp. 032077, 2021, March.
- [30] M. Awais et al., "Novel Framework: Face Feature Selection Algorithm for Neonatal Facial and Related Attributes Recognition," in *IEEE Access*, vol. 8, pp. 59100-59113, 2020, doi: 10.1109/ACCESS.2020.2982865.
- [31] Y. Zhong, W. Deng, J. Hu, D. Zhao, X. Li and D. Wen, "SFace: Sigmoid-Constrained Hypersphere Loss for Robust Face Recognition," in *IEEE Transactions on Image Processing*, vol. 30, pp. 2587-2598, 2021, doi: 10.1109/TIP.2020.3048632.
- [32] A. Elmahmudi and H. Ugail, "Deep Face Recognition using Imperfect Facial Data", *Future Generation Computer Systems*, vol. 99, pp. 213-225, 2019. doi: 10.1016/j.future.2019.04.025, ISSN 0167-739X.
- [33] G. Liu and Q. Zhang, "Mask Wearing Detection Algorithm Based on Improved Tiny YOLOv3", *International Journal of Pattern Recognition and Artificial Intelligence*, pp. 2155007, 2021.
- [34] H. Zhao et al., "Intelligent Diagnosis Using Continuous Wavelet Transform and Gauss Convolutional Deep Belief Network," in *IEEE Transactions on Reliability*, 2022, doi: 10.1109/TR.2022.3180273.
- [35] S. Suganatham, C. Babu and M. Raju, "A Quantitative Evaluation of Change Impact Reachability and Complexity Across Versions of Aspect Oriented Software", *International Arab Journal of Information Technology (IAJIT)*, vol. 14, no. 1, 2017.
- [36] T. P. Majumdar, S. Chhabra, R. Singh and M. Vatsa, "Recognizing Injured Faces via SCIFI Loss," in *IEEE Transactions on Biometrics, Behavior, and Identity Science*, vol. 3, no. 1, pp. 112-123, Jan. 2021, doi: 10.1109/TBIOM.2020.3047274.
- [37] A. Sepas-Moghaddam, M. A. Haque, P. L. Correia, K. Nasrollahi, T. B. Moeslund and F. Pereira, "A Double-Deep Spatio-Angular Learning Framework for Light Field-Based Face Recognition," in *IEEE Transactions on Circuits and Systems for Video Technology*, vol. 30, no. 12, pp. 4496-4512, Dec. 2020, doi: 10.1109/TCSVT.2019.2916669.
- [38] M. Khosravy, K. Nakamura, Y. Hirose, N. Nitta and N. Babaguchi, "Model Inversion Attack by Integration of Deep Generative Models: Privacy-Sensitive Face Generation From a Face Recognition System," in *IEEE Transactions on Information Forensics and Security*, vol. 17, pp. 357-372, 2022, doi: 10.1109/TIFS.2022.3140687.
- [39] A. Kar, S. Pramanik, A. Chakraborty, D. Bhattacharjee, E. S. L. Ho and H. P. H. Shum, "LMZMPM: Local Modified Zernike Moment Per-Unit Mass for Robust Human Face Recognition," in *IEEE Transactions on Information Forensics and Security*, vol. 16, pp. 495-509, 2021, doi: 10.1109/TIFS.2020.3015552.
- [40] R. Liu, Y. Liu, Z. Wang and H. Tian, "Research on face recognition technology based on an improved LeNet-5 system," 2022 International Seminar on Computer Science and Engineering Technology (SCSET), Indianapolis, IN, USA, 2022, pp. 121-123, doi: 10.1109/SCSET55041.2022.00036.
- [41] Liu T, Yang B, Geng Y and Du S (2021) Research on Face Recognition and Privacy in China—Based on Social Cognition and Cultural Psychology. *Front. Psychol.* 12:809736. doi: 10.3389/fpsyg.2021.809736.